

Evidence of Microbursts Observed Near the Equatorial Plane in the Outer Van Allen Radiation Belt

Mykhaylo Shumko^{1,2}, Drew L. Turner², T. P. O'Brien², Seth G. Claudepierre², John Sample¹, D. P. Hartley³, Joseph Fennell², J. Bernard Blake², Matina Gkioulidou⁴, and Donald G. Mitchell⁴

¹Department of Physics, Montana State University, Bozeman, Montana, USA

²Space Science Applications Laboratory, The Aerospace Corporation, Los Angeles, California, USA

³Department of Physics and Astronomy, The University of Iowa, Iowa City, Iowa, USA

⁴Johns Hopkins University Applied Physics Laboratory, Laurel, Maryland, USA

Key Points:

- First report of direct observation of microbursts at high altitude, near the equatorial plane.
- Microbursts' duration, flux enhancement, and energy spectra are similar to prior observations in LEO.
- Microburst generation is not consistent with a single quasi-linear gyroresonant interaction with chorus waves.

Abstract

We present the first evidence of electron microbursts observed near the equatorial plane in Earth's outer radiation belt. We observed the microbursts on March 31st, 2017 with the Magnetic Electron Ion Spectrometer and RBSP Ion Composition Experiment on the Van Allen Probes. Microburst electrons with kinetic energies of 29-92 keV were scattered over a substantial range of pitch angles, and over time intervals of 150-500 ms. Furthermore, the microbursts arrived without dispersion in energy, indicating that they were recently scattered near the spacecraft. We have applied the relativistic theory of wave-particle resonant diffusion to the calculated phase space density, revealing that the observed transport of microburst electrons is not consistent with the hypothesized quasi-linear approximation.

1 Introduction

Since the Van Allen radiation belts were discovered by *Van Allen* [1959] and *Vernov and Chudakov* [1960], decades of work has focused on understanding their origins and effects on the near-Earth space environment and ionosphere-thermosphere system. The energy content of the outer belt is dominated by energetic electrons, with dynamics controlled by a complex interplay between various source and loss mechanisms. One important loss and acceleration mechanism is gyroresonant diffusion in energy and pitch angle (PA) due to scattering of electrons by plasma waves [e.g. *Thorne and Andreoli*, 1981; *Walker*, 1993; *Summers et al.*, 1998; *Meredith et al.*, 2002; *Horne and Thorne*, 2003; *Thorne et al.*, 2005; *Millan and Thorne*, 2007; *Bortnik et al.*, 2008].

Chorus waves are commonly associated with PA and energy diffusion. These waves are typically generated by substorm injections into the inner magnetosphere, which lead to a temperature anisotropy of the source electrons with energies up to tens of keV [e.g. *Horne et al.*, 2003; *Li et al.*, 2009a]. Since these source electrons drift eastward, chorus is most frequently observed in the dawn sector, but it has been observed at all magnetic local times (MLT) [*Li et al.*, 2009b]. Chorus waves are believed to generate electron microburst precipitation through wave-particle interactions.

Microbursts are typically defined as an increase of electron flux in or near the atmospheric loss cone that last < 1 s [e.g. *Anderson and Milton*, 1964; *Blake et al.*, 1996; *Lorentzen et al.*, 2001a]. Empirical and theoretical analyses indicate that microbursts are an important loss process since they can substantially deplete the radiation belt electrons on the order of one day [e.g. *Lorentzen et al.*, 2001b; *O'Brien et al.*, 2004; *Thorne et al.*, 2005; *Breneman et al.*, 2017]. Previously, microbursts have been observed in the upper atmosphere in the form of bremsstrahlung X-rays [e.g. *Parks*, 1967; *Woodger et al.*, 2015; *Anderson et al.*, 2017] and directly in low Earth orbit (LEO) [e.g. *Nakamura et al.*, 1995, 2000; *Blake et al.*, 1996; *Lorentzen et al.*, 2001a,b; *O'Brien et al.*, 2003, 2004; *Lee et al.*, 2005, 2012; *Blum et al.*, 2015; *Crew et al.*, 2016; *Breneman et al.*, 2017; *Mozer et al.*, 2018].

We observed for the first time, microburst-like signatures near their hypothesized origin within the heart of the outer radiation belt. The unique microburst observations we report here were possible with the Van Allen Probe-A's (RBSP-A) Magnetic Electron Ion Spectrometer's (MagEIS) fast sampling rate (~11 ms), and RBSP Ion Composition Experiment's (RBSPICE) PA coverage. The observed microbursts' duration, energy spectra, and energy dispersion signature were similar to microbursts previously reported from LEO. Furthermore, we simultaneously observed structureless "hiss-like" whistler mode wave power in the lower band chorus frequency range [*Li et al.*, 2012]. From previous observations in LEO [e.g. *Blake et al.*, 1996], it is believed that microbursts result from the impulsive scattering of electrons into or near the loss cone, which is on the order of a few tens of degrees in LEO. With this assumption, high altitude microburst observations near the magnetic equator should be very difficult to make since the atmospheric loss cone there is only a few degrees wide. Thus, the loss cone is smaller than the angular resolution

of most particle detectors. Even when an instrument is observing the loss cone, the instrument's field of view will include some portion of the trapped population. The trapped electron flux is typically orders of magnitude higher than that in the loss cone, so that microbursts scattered into the loss cone will be obscured. We present observational evidence that suggests that the sudden impulse of electrons studied here is consistent with the creation of microbursts. Furthermore, these microbursts were scattered over a broad PA range outside of the loss cone, though the loss cone was not directly observed by MagEIS and RBSICE.

This paper explores the properties of the observed microbursts by utilizing in-situ RBSP measurements of waves and particles. This unique high altitude point of view enables us to test whether the observed microburst scattering is consistent with a quasi-linear diffusion process. We have tested this hypothesis with in-situ electron phase space density (PSD) measurements and the relativistic theory of wave-particle resonant diffusion [Walker, 1993; Summers *et al.*, 1998] to determine if the microburst electrons diffused in PA and energy.

2 Spacecraft Instrumentation

NASA's RBSP mission [Mauk *et al.*, 2013], launched on August 30th, 2012, consists of a pair of identically instrumented spacecraft. Their orbit and instrumentation are uniquely configured to enrich our understanding of the particles and waves in the inner magnetosphere. The RBSP spacecraft are in highly elliptical, low-inclination orbit, with perigee of \sim 600 km and apogee of \sim 30,000 km altitude. Their attitude is maintained by spin-stabilization with a period of \sim 11 s and the spin axis is roughly sun-pointing. In this analysis, energetic electron measurements from MagEIS [Blake *et al.*, 2013] and RBSPICE [Mitchell *et al.*, 2013] were used, complemented by magnetic field and wave measurements from Electric and Magnetic Field Instrument and Integrated Science (EMFISIS) [Kletzing *et al.*, 2013].

We observed these microbursts with RBSP-A's MagEIS low energy instrument (MagEIS-A) which measures 20-240 keV electrons. It has an angular acceptance of $3^\circ - 10^\circ$ in the spacecraft spin plane, and 20° perpendicular to the spin plane. MagEIS-A has a high rate data mode which samples at 1000 angular sectors per spacecraft spin (11 ms cadence). MagEIS low on RBSP-B on the other hand samples at 64 angular sectors per spacecraft spin (172 ms cadence), so it was only used for context.

To expand the PA coverage of MagEIS-A, we used the RBSPICE-A time-of-flight instrument. RBSPICE-A measures electron energies in the range of 19 keV - 1 MeV with a fan of six telescopes (the sixth telescope is used only for calibration and was excluded from this analysis). These telescopes have an overall acceptance angle of 160° by 12° which allows them to simultaneously sample a substantial part of the Pitch Angle Distribution (PAD). RBSPICE-A gathers data over 32 sectors per spacecraft spin (\approx 310 ms cadence) and each sector is divided into three sub-sectors corresponding to three measurement modes [Manweiler and Zwiener, 2018]. At the time of the observation, the sub-sector used for electron measurements had an accumulation time of 77 ms. We used RBSPICE-A's Electron Basic Rate (EBR) telemetry data in this analysis which is not averaged, though it is an integral energy channel.

To understand the dynamics of the local magnetic field, we used the EMFISIS instrument. EMFISIS provides measurements of the DC magnetic field with flux gate magnetometers. In addition, it measures electromagnetic waves from 10 Hz to 500 kHz with search coil magnetometers. The spectral matrix and burst data products used in this analysis were from the EMFISIS waveform receiver (WFR) (10 Hz - 12 kHz) and the high frequency receiver (10 kHz - 500 kHz). Burst data were selectively captured at a 35 kHz sample rate, and the survey mode spectral matrix data was captured every 6s.

3 Observations

MagEIS-A and RBSPICE-A observed the microburst-like signatures on March 31st, 2017 at $L^* \approx 6$ and $MLT \approx 19$, calculated with the Tsyganenko 2004 magnetic field model [Tsyganenko and Sitnov, 2005]. The magnetosphere was in the recovery phase of a storm, with minimum Dst of -75 nT observed on March 27th. The local electron number density was on the order of 1 cm^{-3} at this time, so both RBSP spacecraft were located outside the plasmasphere. The two spacecraft were separated by 1700 km, at magnetic latitudes $\lambda \approx -19^\circ$ and $\lambda \approx -18^\circ$ for RBSP-A and RBSP-B, respectively.

MagEIS-A observed microburst electron flux (J) at energies $< 92 \text{ keV}$ around 11:17 UT as shown in panel (a) in Fig. 1. For directional information, panel (b) in Fig. 1 shows flux as a function of local pitch angle (α_L) and time for 46-66 keV electrons. Electrons that traveled towards the northern hemisphere had $\alpha_L < 90^\circ$ and southern hemisphere had $\alpha_L > 90^\circ$. The interval between the two vertical dashed black lines contain the four microbursts examined in this study. We observed these microbursts at $\alpha_L < 50^\circ$, but MagEIS-A did not sample into the 0° loss cone.

Figure 1 panel (c) shows the EMFISIS WFR data from RBSP-A. Between 11:17:05 and 11:17:10 UT, we observed an isolated burst of whistler mode wave power in the frequency range $0.1 < \omega < 0.3 \Omega_{ce0}$, where Ω_{ce0} is the equatorial electron gyrofrequency. No individual rising or falling tone elements were observed during this period, and the waves appeared more “hiss-like” [e.g. Li *et al.*, 2012]. This wave was near-parallel propagating (evidence shown in Supplementary Figure S1) and about 10 minutes later, weak chorus rising tone elements were observed (not shown).

Panels (d)-(f) in Fig. 1 are in the same format as panels (a)-(c), but for RBSP-B. An injection or boundary was observed with RBSP-B at 11:16:50 UT and RBSP-A observed a similar feature soon after 11:18 UT (not shown).

A zoomed-in version of Fig. 1 panels (a) and (b) is shown in Fig. 2. Panel (a) shows the four microburst-like signatures observed between 11:17:10 and 11:17:12 UT, at energies up to 92 keV. The observed duration of the microbursts was 150 - 500 ms, and they did not arrive dispersed in energy, which indicates that they were recently scattered near the spacecraft location. We use IRBEM-Lib, a library dedicated to radiation belt modeling [Boscher *et al.*, 2012], to calculate the mirror point altitudes, which were found to be above LEO. Panel (b) shows the RBSPICE-A EBR time series with the group of microbursts observed at the same time as in panel (a). To understand the timing relationship between the MagEIS-A and RBSPICE-A observations, we marked the times when MagEIS-A observed the four microbursts by vertical black arrows in panels (a) and (b). MagEIS-A observed the first microburst $\sim 0.5 \text{ s}$ before RBSPICE-A. The bounce period of locally mirroring, 100 keV electrons was $\sim 0.8 \text{ s}$, so this was unlikely to have been a returning bounce. This evidence confirms that these microburst signatures are packets of electrons and not a boundary moving back and forth at RBSP-A’s location. To understand the PA extent of these microbursts, panel (c) shows the 29-41 keV MagEIS-A J and RBSPICE-A EBR as a function of α_L and time. The microburst J was observed by MagEIS-A between $25^\circ < \alpha_L < 50^\circ$ and RBSPICE-A between $100^\circ < \alpha_L < 160^\circ$, with the highest intensities close to $\alpha_L = 90^\circ$. RBSPICE-A observed a 10-80% enhancement in count rate over those PAs with the evidence presented in Fig. S2.

4 Analysis

First, we estimated the microburst energy spectra. For each microburst shown in Fig. 2, its flux was averaged and baseline subtracted using the method from O’Brien *et al.* [2004] and then fit with an exponential function. The calculated exponential E-folding energy was found to vary between 25 and 35 keV, which is consistent with spectra derived from prior measurements [Datta *et al.*, 1997; Lee *et al.*, 2005, 2012].

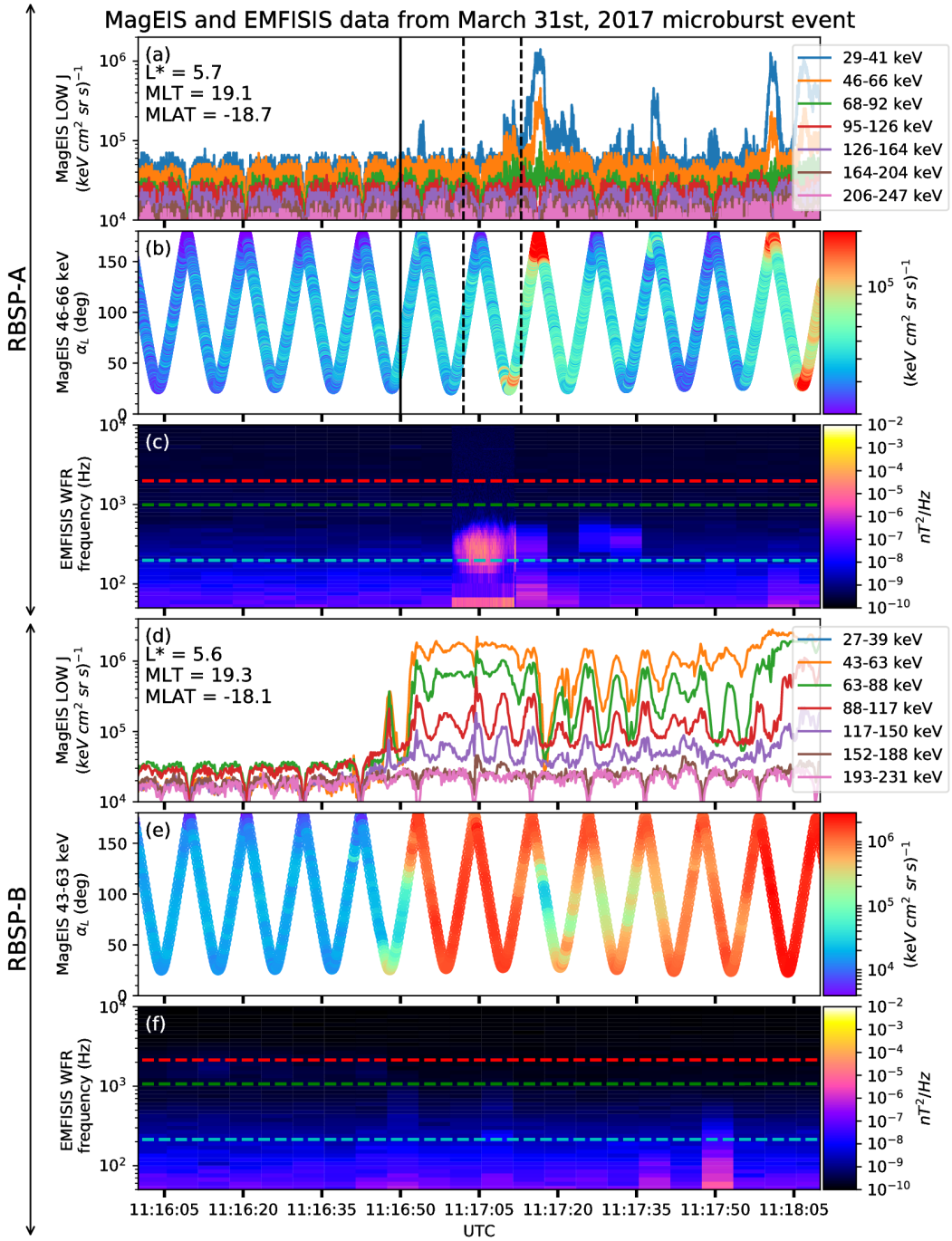


Figure 1. Electron and wave conditions from the MagEIS-A and EMFISIS WFR sensors for the microburst time interval. Panels (a), (b), and (c) are from RBSP-A with its position information annotated in panel (a). Panels (d), (e), and (f) are from RBSP-B with its position information annotated in panel (d). Panel (a) is the MagEIS-A high rate timeseries. Panels (b) and (e) show the evolution of the MagEIS-A J as a function of α_L from the ~ 40 to ~ 60 keV channel. Every 10th point is shown in panel (b). The solid black line in panels (a) and (b) mark the end of the time period used for the PSD fit extrapolation analysis explained in section 4. The dashed black lines in panels (a) and (b) show the time interval used for the observed microburst PSD. Panels (c) and (f) show the EMFISIS WFR spectra, with the available burst data superposed. The red, green, and cyan traces are equatorial f_{ce0} , $f_{ce0}/2$, and $f_{ce0}/10$, respectively.

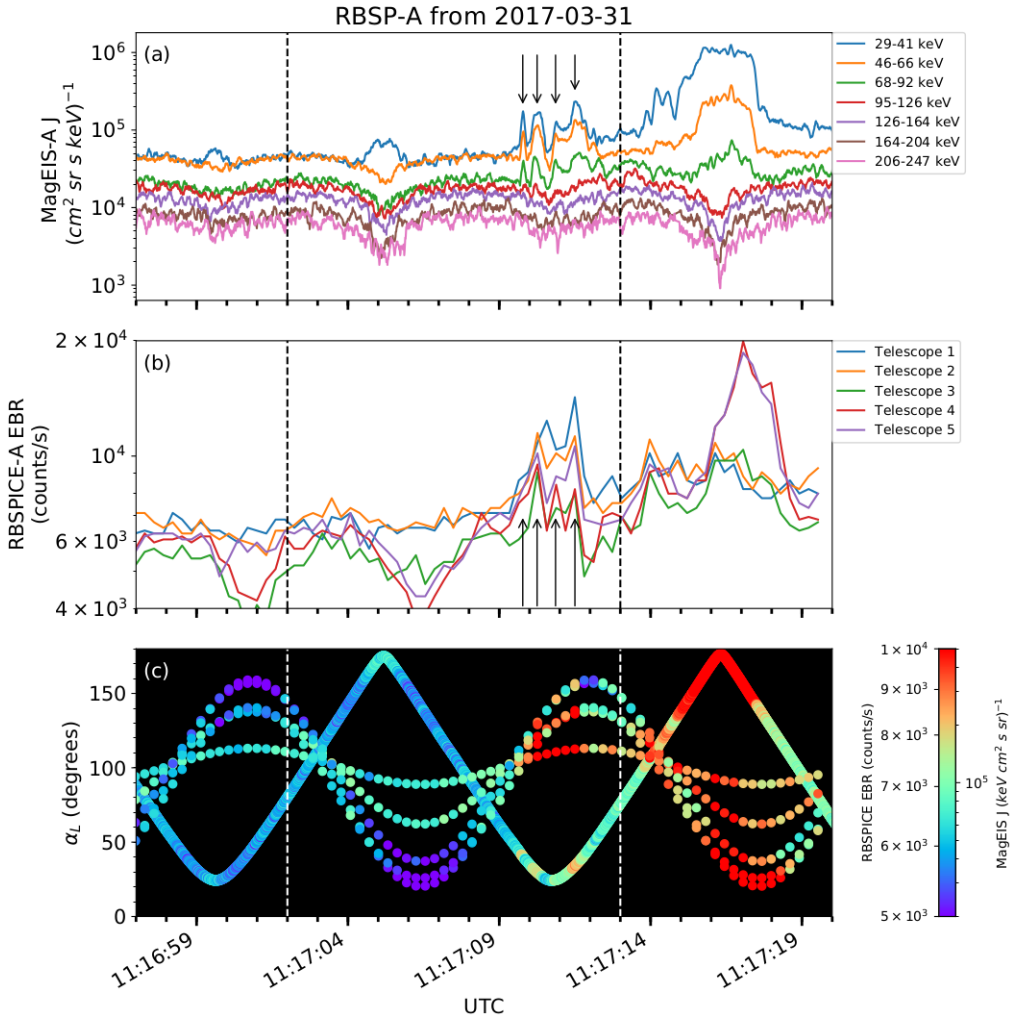


Figure 2. Panel (a) shows the MagEIS-A high rate timeseries. Panel (b) shows the RBSPICE EBR count rate timeseries for > 19 keV electrons. The microbursts were observed between 11:17:10 - 11:17:12 UT and are indicated with the vertical black arrows in panels (a) and (b) for MagEIS-A times. Panel (c) shows the RBSPICE EBR (family of relatively sparse sampled curves) and MagEIS-A J from the 29-41 keV energy channel (single curve) as a function of α_L . The vertical dashed lines show the time interval for the PSD analysis.

We then tested the hypothesis that the microburst electrons were transported in energy and PA by a single chorus wave. We used a procedure similar to sections 3.1 and 4.5 in *Meredith et al.* [2002] which we describe below.

4.1 Microburst and Source PSD

We estimated the electron PSD, $f(p_{\perp}, p_{||})$ where p_{\perp} and $p_{||}$ are the perpendicular and parallel components of the electron momentum relative to the local magnetic field, for the microburst time period. MagEIS-A $J(E, \alpha_L)$ was averaged between 11:17:02 and 11:17:13 UT and binned by α_L into 5° bins. Then, we assumed the conservation of the first adiabatic invariant and mapped α_L to equatorial PA, α_{eq} . The binned $J(E, \alpha_{eq})$ was then converted to $f(p_{\perp}, p_{||})$ via

$$f(p_{\perp}, p_{||}) = \frac{J(E, \alpha_{eq})}{p^2}, \quad (1)$$

where $p = \sqrt{p_{\perp}^2 + p_{||}^2}$. Lastly, α_{eq} was used to separate p into p_{\perp} and $p_{||}$ via

$$\frac{p_{||}}{m_e c} = \frac{\sqrt{E(E + 2E_0)} \cos(\alpha_{eq})}{E_0} \quad (2)$$

$$\frac{p_{\perp}}{m_e c} = \frac{\sqrt{E(E + 2E_0)} \sin(\alpha_{eq})}{E_0} \quad (3)$$

where c is the speed of light, E is the kinetic energy, m_e is the electron mass, and E_0 is the electron rest energy. The observed $f(p_{\perp}, p_{||})$ in dimensionless momentum space is shown in Fig. 3 in all panels between the $p_{||}$ axis and the white dotted lines. The bright spot in $f(p_{\perp}, p_{||})$ in the upper $p_{||}$ plane represents the four microbursts. Along with the observed PSD, we use Fig. 3 to explore the various PSD extrapolation and diffusion model assumptions which are described below.

We proceed under the assumption that the source of the microburst electrons is not likely to be at the latitude of the observation, and is closer to the magnetic equator. To look for a source of microburst electrons, we extrapolate the unobserved $f(p_{\perp}, p_{||})$ of electrons with $|\lambda_m| < 19^{\circ}$ using two cases with a 90° -peaked PAD of the form

$$f(E, \alpha_{eq}) = f_0(E) \sin^n(\alpha_{eq}) \quad (4)$$

where $f_0(E)$ is a scaling parameter and n is a power parameter. Similarly to the in-situ $f(p_{\perp}, p_{||})$, the $f(E, \alpha_{eq}) \mapsto f(p_{\perp}, p_{||})$ conversion was applied.

In the first case, we fitted Eq. 4 to the quiet time $J(E, \alpha_{eq})$ from 11:15:00 to 11:16:50 UT (end time shown as the black vertical line in Fig. 1). The fitted PAD was relatively flat with $0.4 < n < 0.5$ and highest magnitude of f_0 was $0.05 \text{ cm}^3/(\text{MeV})^3$. This extrapolated $f(p_{\perp}, p_{||})$ is shown in Fig. 3 panels (A) and (E), between the dotted white lines for scattering at $\lambda = 0^{\circ}$ and 20° , respectively. To confirm the relatively low n parameter, we found times where RBSP-A was in a similar L-MLT location, but closer to the magnetic equator. At 2 and 19 UT on the same day, we fit the $J(E, \alpha_{eq})$, and the fit parameters were very similar to the pre-microburst $f(p_{\perp}, p_{||})$ at 11 UT. Thus it is a reasonable assumption that $f(p_{\perp}, p_{||})$ was relatively flat near the equator.

In the other case, we estimate how large n would have to be in order to find sufficient PSD in MagEIS-A's energy range to be a source of the microburst electrons. We used $n \in \{1, 2, 4\}$ and we forced the $f_0(E)$ parameter to match the observed $f(p_{\perp}, p_{||})$ at the most equatorial PAs observed by MagEIS-A. These extrapolations are shown in columns 2-4 in Fig. 3. There was enough source PSD anywhere in MagEIS-A's energy range only if $n \geq 2$.

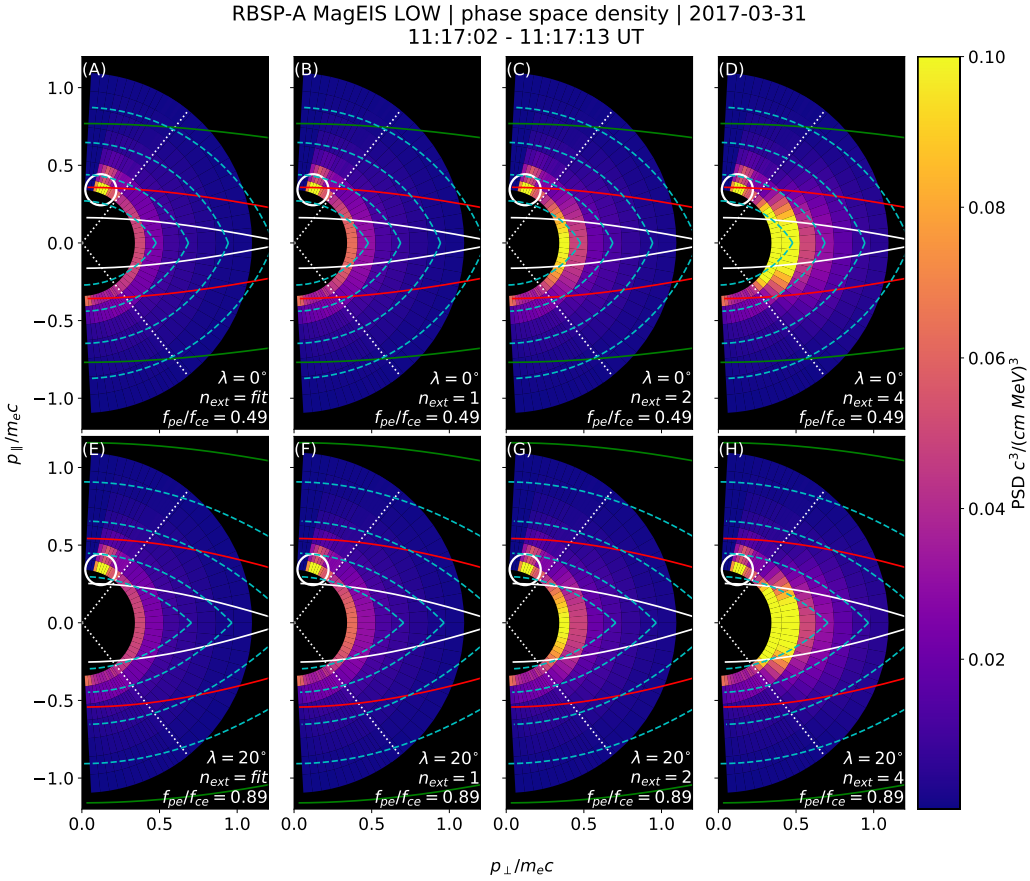


Figure 3. The colored annulus represents $f(p_{\perp}, p_{\parallel})$ in normalized momentum space, parallel and perpendicular to the background magnetic field. The microburst $f(p_{\perp}, p_{\parallel})$ is highlighted with the white circle. The columns show different powers of the sine extrapolation, and rows show the different magnetic latitudes of the scattering. The white dotted traces represent the boundary between the data and extrapolation. The green, red, and white solid traces are the resonance curves for $\omega = 0.2\Omega_{ce}, 0.4\Omega_{ce}, 0.6\Omega_{ce}$, respectively. The cyan dashed traces are the diffusion curves for a $\omega = 0.4\Omega_{ce}$ wave (waves of other frequency have similar diffusion curves). The magnetic latitude of the scattering, the ratio of the plasma to the cyclotron frequency, and the power of the sine extrapolation is annotated in each panel. For the resonance and diffusion curves, the density model assumed a $n_L = 1 e^-/cm^3$ and $\psi = -1$.

4.2 Motion of resonant electrons in phase space

To calculate the motion of resonant electrons in momentum space, we used the relativistic theory of wave-particle resonant diffusion developed by *Walker* [1993] and *Summers et al.* [1998] and applied in *Meredith et al.* [2002]. The chorus wave can modify $f(p_{\perp}, p_{\parallel})$ when a resonance condition is satisfied. The cyclotron resonance condition between an electron with velocity $v = \sqrt{v_{\parallel}^2 + v_{\perp}^2}$ and a parallel propagating wave of frequency ω and wave number k_{\parallel} is given by

$$\omega - v_{\parallel} k_{\parallel} = \frac{\Omega_{ce}}{\gamma}, \quad (5)$$

where Ω_{ce} is the electron gyrofrequency at the scattering location, and γ is the relativistic correction. Assuming the cold plasma approximation,

$$k_{\parallel} = \frac{\omega}{c} \sqrt{1 - \frac{\omega_{pe}^2}{\omega(\omega - |\Omega_{ce}|)}}, \quad (6)$$

where ω_{pe} is the plasma frequency. For a particular set of parameters, Eq. 5 defines a curve in momentum space that describes which electrons will resonate with a monochromatic wave.

To calculate k_{\parallel} , we approximated the electron number density, $n_e(\lambda)$ locally and at the magnetic equator. Locally, the plasma density was approximately $n_e(\lambda = -20^\circ) = n_L \approx 1 \text{ cm}^{-3}$. We used magnetospheric seismology techniques [e.g. *Takahashi and Denton*, 2007] to parameterize $n_e(\lambda)$ elsewhere along the field line with

$$n_e(\lambda) = n_e(0) \left(\frac{LR_e}{R(\lambda)} \right)^{\psi} \quad (7)$$

where R_e is the Earth's radius, $R(\lambda)$ is the radial distance from the Earth to the spacecraft, and ψ is the exponent parameter. Assuming a dipole magnetic field for which $R(\lambda) = LR_e \cos^2 \lambda$ [e.g. *Schulz and Lanzerotti*, 1974], we can express Eq. 7 in terms of n_L via

$$n_e(\lambda) = n_L \left(\frac{\cos \lambda_L}{\cos \lambda} \right)^{2\psi} \quad (8)$$

where we used $\psi = -1$ (higher density at the magnetic equator) in this analysis. We chose this exponent parameter because it is a realistic best case scenario for the electrons to be transported along the diffusion curves (described below).

Walker [1993] and *Summers et al.* [1998] argued that a resonant electron will move along diffusion curves in momentum space. A diffusion curve is derived as follows. In the reference frame moving with a monochromatic chorus wave's phase velocity (wave frame), the chorus wave is stationary and there is no electric field. Thus in the wave frame, the electron's kinetic energy is conserved, and the electron's velocity in the wave frame can be expressed in differential form as

$$v_{\parallel} dv_{\parallel} + v_{\perp} dv_{\perp} = 0. \quad (9)$$

After a Lorentz transformation of Eq. 9 into the magnetospheric frame, kinetic energy will no longer be conserved. After integration and manipulation of Eq. 9, we obtain:

$$\left(1 - \frac{u_0^2 v_0^2}{c^4}\right) v_{\parallel}^2 - 2u_0 \left(1 - \frac{v_0^2}{c^2}\right) v_{\parallel} + \left(1 - \frac{u_0^2}{c^2}\right) v_{\perp}^2 = v_0^2 - u_0^2 \quad (10)$$

where $u_0 = \omega/k_{\parallel}$ is the phase velocity, and v_0 is a constant of integration [*Walker*, 1993; *Summers et al.*, 1998]. Equation 10 defines a family of diffusion curves in momentum space on which resonant electrons will move. The distance that an electron moves along a diffusion curve is a function of wave and plasma parameters, and is estimated from the magnitude of the diffusion coefficients and the resonance time.

4.3 Comparing the microburst PSD to diffusion theory

Superposed on the PSD plots in Fig. 3 are resonance curves for chorus waves of $\omega = 0.2\Omega_{ce}$, $0.4\Omega_{ce}$, $0.6\Omega_{ce}$ and a few diffusion curves for a $\omega = 0.4\Omega_{ce}$ wave. These curves were parameterized by λ using a dipole magnetic field for $\lambda = 0^\circ$ (Fig. 3, panels A-D) and $\lambda = 20^\circ$ (Fig. 3, panels E-H). If the transport of microburst electrons is consistent with gyro-resonant diffusion, a diffusion curve that passes through the microburst $f(p_\perp, p_\parallel)$ must also pass through another region with at least the same magnitude PSD ($f(p_\perp, p_\parallel) \geq 0.1 \text{ c}^3/(\text{cm MeV})^3$) e.g. Fig. 3, panel (D). With this constraint, an artificially high extrapolated $f(p_\perp, p_\parallel)$ with $n > 2$ (5 times larger than calculated from the fits) must be assumed for there to have been a sufficient source of PSD anywhere in MagEIS-A's energy range.

We now show that by comparing MagEIS observations with theory, that the minimum wave amplitude necessary to scatter these electrons is much higher than was observed by EMFISIS-A. If we assume a unrealistic PAD with enough PSD just equatorward of RBSP-A, we can use MagEIS-A observations to calculate the minimum $\Delta\alpha_{eq}$ that the electrons were transported. We then used diffusion theory to calculate the necessary wave amplitude. For microbursts with larger PAs, MagEIS-A observed a transport of $\Delta\alpha_{eq} = 9^\circ$ and for microbursts with smaller PAs, the observed transport was $\Delta\alpha_{eq} = 24^\circ$. The required wave amplitude was calculated with Eq. 3 from *Thorne and Andreoli* [1981] assuming a maximum resonance period of a quarter bounce. The observed change in PA requires a wave amplitude $0.2 < |B_w| < 0.5 \text{ nT}$. For a few brief moments, the EMFISIS-A WFR waveform data showed $0.1 < |B_w| < 0.15 \text{ nT}$, so a transport of 9° is plausible, but not likely for 24° .

Another source of microburst electrons may be from energies below MagEIS-A's range. The Helium, Oxygen, Proton, and Electron mass spectrometer [Funsten *et al.*, 2013] on RBSP-A observed $f(p_\perp, p_\parallel) \geq 0.1 \text{ c}^3/(\text{cm MeV})^3$ for $< 23 \text{ keV}$ electrons at this time. We then assumed the wave amplitude derived above to predict the transport in energy. We used the fact that the momentum and pitch angle diffusion coefficients, D_{pp} and $D_{\alpha\alpha}$ are related via $D_{pp}/p^2 \sim D_{\alpha\alpha}$ or equivalently, $\Delta p/p \sim \Delta\alpha$. The observed PA transport corresponds to an energy transport of $6 < \Delta E < 16 \text{ keV}$. Therefore, this wave can transport 23 keV electrons from smaller pitch angles to larger pitch angles and would be observed in the 29 – 41 keV MagEIS-A channel. However, this wave is insufficient to transport electrons to the 68 – 92 keV channel in one interaction. Therefore we conclude that quasi-linear diffusion cannot explain the observed microbursts.

5 Discussion and Conclusions

These novel observations of impulsive electron signatures reported here fall well within the broad definition of a microburst as described in section 1. Their properties were similar to microbursts observed in LEO, with an E-folding energy of $25 < E_0 < 35 \text{ keV}$ [Datta *et al.*, 1997; Lee *et al.*, 2005, 2012], duration of 150-500 ms [Lorentzen *et al.*, 2001a], observed upper energy limit of 92 keV, and a lack of clear energy dispersion [Breneman *et al.*, 2017]. With MagEIS-A's high time and energy resolution, we conclude that these dispersionless microbursts were recently scattered near the spacecraft. Furthermore, RBSPICE-A's PA coverage suggests that these electrons were scattered over a substantial range of PAs, with the highest intensities near $\alpha_L = 90^\circ$. Overall, our observational evidence suggests that on time scales shorter than one bounce period, the chorus wave effectively accelerated trapped electrons over a broad PA range.

In the theoretical framework of wave-particle resonant diffusion applied to the observed PSD in section 4, we determine that the observed scattering is not consistent with the quasi-linear approximation. The nearest source of sufficient PSD is too far away in phase space to have been transported by the hypothesized quasi-linear process over a timescale

shorter than one bounce period (one interaction). A similar conclusion was made by *Mozer et al.* [2018] who used quasi-linear theory constrained by RBSP wave measurements. They successfully modeled the one second average precipitating flux observed with AeroCube-6 (AC-6) CubeSats during a conjunction, but they were unable to model the AC-6 fluxes on smaller time scales.

To put these microburst observations into a wider magnetospheric perspective, we observed them during the recovery phase of a minimum Dst of -75 nT storm, a statistically favorable time period for microbursts [*O'Brien et al.*, 2003]. Furthermore, during the same storm on March 27th, the Arase spacecraft observed highly correlated lower band chorus with 10-50 keV electron precipitation inside the loss cone. At that time, Arase's magnetic field footprint was near The Pas All-Sky Imager (part of the THEMIS mission) which simultaneously observed pulsating auroral patches [*Kasahara et al.*, 2018]. While microbursts and pulsating auroral patches have not been clearly connected, they are both believed to be a product of electron scattering by whistler mode waves [e.g. *Lorentzen et al.*, 2001a; *O'Brien et al.*, 2003; *Nishimura et al.*, 2011; *Ozaki et al.*, 2012].

The combined capabilities of the various RBSP wave and particle instruments enable comprehensive studies of wave-particle scattering and the resulting microburst precipitation. From a preliminary search by the authors, other microburst-like signatures have been found with RBSP. Similar to previous studies [e.g. *O'Brien et al.*, 2003; *Blum et al.*, 2015], a statistical study of high-altitude microbursts in L-MLT space needs to be conducted before we can verify that these microbursts are the counterpart of the microbursts observed in LEO and the upper atmosphere.

Acknowledgments

The authors acknowledge the technicians, engineers, and scientists who made the RBSP and AC-6 missions possible. One author (Shumko) would like to acknowledge Dana Longcope for his help in understanding the quasi-linear diffusion theory. Dr. Gkioulidou was supported by JHU/APL subcontract 131803 to the NJIT under NASA Prime contract NNN06AA01C. EMFISIS work was supported by JHU/APL contract no. 921647 under NASA Prime contract No. NAS5-01072. The MagEIS instrument was funded by NASA's Prime contract no. NAS5-01072. The level 3 MagEIS-A "high rate" data is available in the Supporting Information, level 1 RBSPICE EBR data is archived at <http://rbspicea.ftecs.com/>, and the EMFISIS level 2 spectral matrix and burst data as well as the level 3 magnetometer data is archived at <http://emfisis.physics.uiowa.edu/data/index>. The IRBEM Library can be obtained at irbem.sf.net.

References

- Abel, B., and R. M. Thorne (1998), Electron scattering loss in earth's inner magnetosphere: 1. dominant physical processes, *Journal of Geophysical Research: Space Physics*, 103(A2), 2385–2396.
- Anderson, B., S. Shekhar, R. Millan, A. Crew, H. Spence, D. Klumpar, J. Blake, T. O'Brien, and D. Turner (2017), Spatial scale and duration of one microburst region on 13 August 2015, *Journal of Geophysical Research: Space Physics*.
- Anderson, K. A., and D. W. Milton (1964), Balloon observations of X rays in the auroral zone: 3. High time resolution studies, *Journal of Geophysical Research*, 69(21), 4457–4479, doi:10.1029/JZ069i021p04457.
- Blake, J., M. Looper, D. Baker, R. Nakamura, B. Klecker, and D. Hovestadt (1996), New high temporal and spatial resolution measurements by sampex of the precipitation of relativistic electrons, *Advances in Space Research*, 18(8), 171 – 186, doi: [http://dx.doi.org/10.1016/0273-1177\(95\)00969-8](http://dx.doi.org/10.1016/0273-1177(95)00969-8).
- Blake, J., P. Carranza, S. Claudepierre, J. Clemmons, W. Crain, Y. Dotan, J. Fennell, F. Fuentes, R. Galvan, J. George, et al. (2013), The magnetic electron ion spectrometer

- (MagEIS) instruments aboard the radiation belt storm probes (RBSP) spacecraft, *Space Science Reviews*, 179(1-4), 383–421.
- Blum, L., X. Li, and M. Denton (2015), Rapid MeV electron precipitation as observed by SAMPEX/HILT during high-speed stream-driven storms, *Journal of Geophysical Research: Space Physics*, 120(5), 3783–3794, doi:10.1002/2014JA020633, 2014JA020633.
- Bortnik, J., R. Thorne, and U. S. Inan (2008), Nonlinear interaction of energetic electrons with large amplitude chorus, *Geophysical Research Letters*, 35(21).
- Boscher, D., S. Bourdarie, P. O'Brien, T. Guild, and M. Shumko (2012), Irbem-lib library.
- Breneman, A., A. Crew, J. Sample, D. Klumpar, A. Johnson, O. Agapitov, M. Shumko, D. Turner, O. Santolik, J. Wygant, et al. (2017), Observations directly linking relativistic electron microbursts to whistler mode chorus: Van allen probes and FIREBIRD II, *Geophysical Research Letters*.
- Crew, A. B., H. E. Spence, J. B. Blake, D. M. Klumpar, B. A. Larsen, T. P. O'Brien, S. Driscoll, M. Handley, J. Legere, S. Longworth, K. Mashburn, E. Mosleh, N. Ryha-jlo, S. Smith, L. Springer, and M. Widholm (2016), First multipoint in situ observations of electron microbursts: Initial results from the NSF FIREBIRD II mission, *Journal of Geophysical Research: Space Physics*, 121(6), 5272–5283, doi:10.1002/2016JA022485, 2016JA022485.
- Datta, S., R. Skoug, M. McCarthy, and G. Parks (1997), Modeling of microburst electron precipitation using pitch angle diffusion theory, *Journal of Geophysical Research: Space Physics*, 102(A8), 17,325–17,333.
- Douma, E., C. J. Rodger, L. W. Blum, and M. A. Clilverd (2017), Occurrence characteristics of relativistic electron microbursts from SAMPEX observations, *Journal of Geophysical Research: Space Physics*, 122(8), 8096–8107, doi:10.1002/2017JA024067, 2017JA024067.
- Drake, J., O. Agapitov, and F. Mozer (2015), The development of a bursty precipitation front with intense localized parallel electric fields driven by whistler waves, *Geophysical Research Letters*, 42(8), 2563–2570.
- Funsten, H., R. Skoug, A. Guthrie, E. MacDonald, J. Baldonado, R. Harper, K. Henderson, K. Kihara, J. Lake, B. Larsen, et al. (2013), Helium, Oxygen, Proton, and Electron (HOPE) mass spectrometer for the radiation belt storm probes mission, *Space Science Reviews*, 179(1-4), 423–484.
- Horne, R., R. Thorne, N. Meredith, and R. Anderson (2003), Diffuse auroral electron scattering by electron cyclotron harmonic and whistler mode waves during an isolated sub-storm, *Journal of Geophysical Research: Space Physics*, 108(A7).
- Horne, R. B., and R. M. Thorne (2003), Relativistic electron acceleration and precipitation during resonant interactions with whistler-mode chorus, *Geophysical Research Letters*, 30(10), doi:10.1029/2003GL016973, 1527.
- Kasahara, S., Y. Miyoshi, S. Yokota, T. Mitani, Y. Kasahara, S. Matsuda, A. Kumamoto, A. Matsuoka, Y. Kazama, H. Frey, et al. (2018), Pulsating aurora from electron scattering by chorus waves, *Nature*, 554(7692), 337.
- Kletzing, C., W. Kurth, M. Acuna, R. MacDowall, R. Torbert, T. Averkamp, D. Bodet, S. Bounds, M. Chutter, J. Connerney, et al. (2013), The electric and magnetic field instrument suite and integrated science (EMFISIS) on RBSP, *Space Science Reviews*, 179(1-4), 127–181.
- Lee, J.-J., G. K. Parks, K. W. Min, H. J. Kim, J. Park, J. Hwang, M. P. McCarthy, E. Lee, K. S. Ryu, J. T. Lim, E. S. Sim, H. W. Lee, K. I. Kang, and H. Y. Park (2005), Energy spectra of 170–360 keV electron microbursts measured by the korean STSAT-1, *Geophysical Research Letters*, 32(13), doi:10.1029/2005GL022996, 113106.
- Lee, J. J., G. K. Parks, E. Lee, B. T. Tsurutani, J. Hwang, K. S. Cho, K.-H. Kim, Y. D. Park, K. W. Min, and M. P. McCarthy (2012), Anisotropic pitch angle distribution of 100 keV microburst electrons in the loss cone: measurements from STSAT-1, *Annales Geophysicae*, 30(11), 1567–1573, doi:10.5194/angeo-30-1567-2012.

- Li, W., R. Thorne, V. Angelopoulos, J. Bonnell, J. McFadden, C. Carlson, O. LeContel, A. Roux, K. Glassmeier, and H. Auster (2009a), Evaluation of whistler-mode chorus intensification on the nightside during an injection event observed on the THEMIS spacecraft, *Journal of Geophysical Research: Space Physics*, 114(A1).
- Li, W., R. M. Thorne, V. Angelopoulos, J. Bortnik, C. M. Cully, B. Ni, O. LeContel, A. Roux, U. Auster, and W. Magnes (2009b), Global distribution of whistler-mode chorus waves observed on the THEMIS spacecraft, *Geophysical Research Letters*, 36(9), doi:10.1029/2009GL037595, 109104.
- Li, W., R. Thorne, J. Bortnik, X. Tao, and V. Angelopoulos (2012), Characteristics of hiss-like and discrete whistler-mode emissions, *Geophysical Research Letters*, 39(18).
- Lorentzen, K. R., J. B. Blake, U. S. Inan, and J. Bortnik (2001a), Observations of relativistic electron microbursts in association with VLF chorus, *Journal of Geophysical Research: Space Physics*, 106(A4), 6017–6027, doi:10.1029/2000JA003018.
- Lorentzen, K. R., M. D. Looper, and J. B. Blake (2001b), Relativistic electron microbursts during the GEM storms, *Geophysical Research Letters*, 28(13), 2573–2576, doi:10.1029/2001GL012926.
- Manweiler, J. W., and H. M. Zwiener (2018), Science Operations Center (SOC) RBSPICE Science Data Handbook Revision: e, *Tech. rep.*, Fundamental Technologies, LLC.
- Mauk, B., N. J. Fox, S. Kanekal, R. Kessel, D. Sibeck, and A. Ukhorskiy (2013), Science objectives and rationale for the radiation belt storm probes mission, *Space Science Reviews*, 179(1-4), 3–27.
- Meredith, N., R. Horne, D. Summers, R. Thorne, R. Iles, D. Heynderickx, and R. Anderson (2002), Evidence for acceleration of outer zone electrons to relativistic energies by whistler mode chorus, in *Annales Geophysicae*, vol. 20, pp. 967–979.
- Millan, R., and R. Thorne (2007), Review of radiation belt relativistic electron losses, *Journal of Atmospheric and Solar-Terrestrial Physics*, 69(3), 362 – 377, doi: <http://dx.doi.org/10.1016/j.jastp.2006.06.019>.
- Mitchell, D., L. Lanzerotti, C. Kim, M. Stokes, G. Ho, S. Cooper, A. Ukhorskiy, J. Manweiler, S. Jaskulek, D. Haggerty, et al. (2013), Radiation belt storm probes ion composition experiment (RBSPICE), *Space Science Reviews*, 179(1-4), 263–308.
- Mozer, F. S., O. V. Agapitov, J. B. Blake, and I. Y. Vasko (2018), Simultaneous observations of lower band chorus emissions at the equator and microburst precipitating electrons in the ionosphere, *Geophysical Research Letters*, doi:10.1002/2017GL076120.
- Nakamura, R., D. N. Baker, J. B. Blake, S. Kanekal, B. Klecker, and D. Hovestadt (1995), Relativistic electron precipitation enhancements near the outer edge of the radiation belt, *Geophysical Research Letters*, 22(9), 1129–1132, doi:10.1029/95GL00378.
- Nakamura, R., M. Isowa, Y. Kamide, D. Baker, J. Blake, and M. Looper (2000), Observations of relativistic electron microbursts in association with VLF chorus, *J. Geophys. Res.*, 105, 15,875–15,885.
- Nishimura, Y., J. Bortnik, W. Li, R. Thorne, L. Chen, L. Lyons, V. Angelopoulos, S. Mende, J. Bonnell, O. Le Contel, et al. (2011), Multievent study of the correlation between pulsating aurora and whistler mode chorus emissions, *Journal of Geophysical Research: Space Physics*, 116(A11).
- O'Brien, T. P., K. R. Lorentzen, I. R. Mann, N. P. Meredith, J. B. Blake, J. F. Fennell, M. D. Looper, D. K. Milling, and R. R. Anderson (2003), Energization of relativistic electrons in the presence of ULF power and MeV microbursts: Evidence for dual ULF and VLF acceleration, *Journal of Geophysical Research: Space Physics*, 108(A8), doi: 10.1029/2002JA009784.
- O'Brien, T. P., M. D. Looper, and J. B. Blake (2004), Quantification of relativistic electron microburst losses during the GEM storms, *Geophysical Research Letters*, 31(4), doi:10.1029/2003GL018621, 104802.
- Omura, Y., Y. Katoh, and D. Summers (2008), Theory and simulation of the generation of whistler-mode chorus, *Journal of Geophysical Research: Space Physics*, 113(A4).

- Ozaki, M., S. Yagitani, K. Ishizaka, K. Shiokawa, Y. Miyoshi, A. Kadokura, H. Yamagishi, R. Kataoka, A. Ieda, Y. Ebihara, N. Sato, and I. Nagano (2012), Observed correlation between pulsating aurora and chorus waves at Syowa Station in Antarctica: A case study, *Journal of Geophysical Research: Space Physics*, 117(A8), doi: 10.1029/2011JA017478.
- Parks, G. K. (1967), Spatial characteristics of auroral-zone X-ray microbursts, *Journal of Geophysical Research*, 72(1), 215–226.
- Schulz, M., and L. J. Lanzerotti (1974), *Particle Diffusion in the Radiation Belts*, Springer.
- Selesnick, R. S., J. B. Blake, and R. A. Mewaldt (2003), Atmospheric losses of radiation belt electrons, *Journal of Geophysical Research: Space Physics*, 108(A12), doi: 10.1029/2003JA010160, 1468.
- Summers, D., R. M. Thorne, and F. Xiao (1998), Relativistic theory of wave-particle resonant diffusion with application to electron acceleration in the magnetosphere, *Journal of Geophysical Research: Space Physics*, 103(A9), 20,487–20,500.
- Takahashi, K., and R. E. Denton (2007), Magnetospheric seismology using multiharmonic toroidal waves observed at geosynchronous orbit, *Journal of Geophysical Research: Space Physics*, 112(A5).
- Tao, X., J. Bortnik, J. Albert, K. Liu, and R. Thorne (2011), Comparison of quasilinear diffusion coefficients for parallel propagating whistler mode waves with test particle simulations, *Geophysical Research Letters*, 38(6).
- Thorne, R. M., and L. J. Andreoli (1981), *Mechanisms for Intense Relativistic Electron Precipitation*, pp. 381–394, Springer Netherlands, Dordrecht, doi:10.1007/978-94-009-8417-2_31.
- Thorne, R. M., T. P. O'Brien, Y. Y. Shprits, D. Summers, and R. B. Horne (2005), Timescale for MeV electron microburst loss during geomagnetic storms, *Journal of Geophysical Research: Space Physics*, 110(A9), doi:10.1029/2004JA010882, a09202.
- Tsyganenko, N. A., and M. I. Sitnov (2005), Modeling the dynamics of the inner magnetosphere during strong geomagnetic storms, *Journal of Geophysical Research: Space Physics*, 110(A3), doi:10.1029/2004JA010798.
- Van Allen, J. A. (1959), The geomagnetically trapped corpuscular radiation, *Journal of Geophysical Research*, 64(11), 1683–1689, doi:10.1029/JZ064i011p01683.
- Vernov, S., and A. Chudakov (1960), Investigation of radiation in outer space, in *International Cosmic Ray Conference*, vol. 3, p. 19.
- Walker, A. D. M. (1993), *Plasma waves in the magnetosphere*, vol. 24, Springer Science & Business Media.
- Woodger, L., A. Halford, R. Millan, M. McCarthy, D. Smith, G. Bowers, J. Sample, B. Anderson, and X. Liang (2015), A summary of the BARREL campaigns: Technique for studying electron precipitation, *Journal of Geophysical Research: Space Physics*, 120(6), 4922–4935.